ROBUST PIECEWISE LINEAR SHEET CONTROL IN A PRINTER PAPER PATH [1]

Björn Bukkems, Jeroen de Best,
René van de Molengraft, Maarten Steinbuch

Dynamics and Control Technology Group,
Department of Mechanical Engineering
Technische Universiteit Eindhoven,
P.O. Box 513, 5600 MB Eindhoven, The Netherlands
Phone: +31 40 247 2841, Fax: +31 40 246 1418
B.H.M.Bukkems@tue.nl, J.J.T.H.d.Best@student.tue.nl,
M.J.G.v.d.Molengraft@tue.nl, M.Steinbuch@tue.nl

Abstract: This paper presents a control design approach for robust sheet control in a printer paper path. The overall design question is formulated in terms of a hierarchical control set-up with a low level motor control part and a high level sheet control part. The sheet dynamics, subject to disturbances and parameter uncertainties, are captured in the piecewise linear modeling formalism. Based on this model, the control design yields robust sheet feedback controllers and a closed-loop system capable of rejecting disturbances up to a prescribed level. The effectiveness of the control design is shown on an experimental paper path setup.

Keywords: Piecewise Linear Systems, Hierarchical Control, Robust Control, Linear Matrix Inequalities.

1. INTRODUCTION

The design of a reliable sheet handling mechanism is a central issue in the development of today's cut sheet printer paper paths. An example of such a paper path is shown in Figure 1. Sheets enter this paper path at the Paper Input Module (PIM) and are transported to the Image Transfer Station (ITS) where the image is printed onto the sheet at high pressure and high temperature. After the print has been made, sheets can either re-enter the first part of the paper path for back side printing or they can go to the finisher (FIN). The transportation of sheets is done via pinches. A pinch is a set of rollers consisting of two parts: one part that is actuated by a motor and one part that is used to apply sufficient normal force to prevent the sheet from slipping. As can be seen from Figure 1, pinches can be driven either individually or grouped together in sections.

One of the objectives of the printer's sheet handling mechanism is to accurately deliver sheets to the ITS. Each sheet must synchronize with its corresponding image with respect to both the ITS entry time and the constant printing velocity to achieve a high printing quality. One way to realize the desired printing quality is using a high precision mechanical design. An alternative approach is to exploit the power of closed-loop sheet control. In this approach, the tolerances on the mechanical parts of the paper path are allowed

[1] This work has been carried out as part of the Boderc project under the responsibility of the Embedded Systems Institute. This project is partially supported by the Netherlands Ministry of Economic Affairs under the Senter TS program.

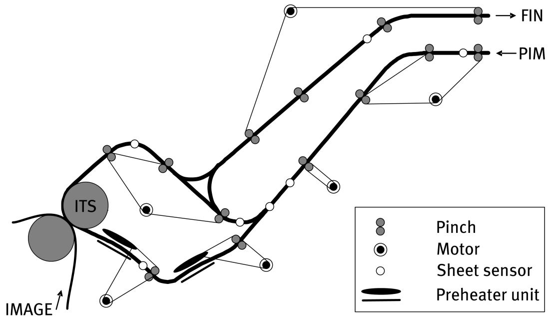

Fig. 1. Schematic representation of a paper path.

to be larger and less effort and money have to be put in constructing a very stiff frame and drive train, since robustness against disturbances and uncertainties in the mechanical design is achieved by sheet feedback control. To realize a sheet feedback control system, the sheet position has to be known. This can, for example, be realized by adding position sensors, possibly in combination with model-based observer techniques.

Known results on sheet feedback control can be found in (Kruciński, 2000; Cloet, 2001; Rai and Jackson, 1998), where robustness against perturbations and disturbances is not taken into account in the control design. In this paper we present a model-based sheet feedback control design procedure that takes into account both system uncertainties and disturbances. Based on the results presented in (Feng, 2002; Chen *et al.*, 2004) we guarantee both stability and performance of the closed-loop system. To synthesize controllers for the sheet tracking problem, we formulate the system in terms of its error dynamics. Experiments will confirm the robustness and disturbance attenuation of the closed-loop system.

The remainder of this paper is organized as follows: in Section 2 the system under consideration will be discussed in more detail and the problem statement will be given. In Section 3 we will discuss the controller design method for the uncertain paper path system that is subject to disturbances. In Section 4 we will present the experimental setup that has been used to validate the proposed control design approach in practice. The validation experiments will be presented in Section 5, and conclusions and recommendations will come at the end.

2. SHEET FEEDBACK CONTROL PROBLEM

In this paper, the focus will be on sheet feedback control design in a basic paper path, shown in Fig 2. By considering this basic version, the essence of the control problem becomes clear. As a result, the switching nature of the system, caused by the consecutive changing of the driving pinch,

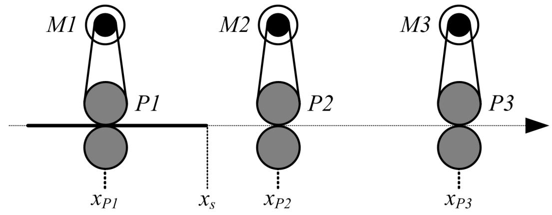

Fig. 2. Schematic representation of the printer paper path.

naturally arises in the control design and a structured design approach can be carried out. Since we consider the motion of sheets only when they are in the paper path, the PIM and FIN are not taken into account. The considered paper path consists of three pinches (*P1*, *P2*, and *P3*) only, each of which is driven by a separate motor (*M1*, *M2*, and *M3*, respectively). The locations of the three pinches in the paper path are represented by x_{P1}, x_{P2}, and x_{P3}, respectively. These locations are chosen such that the distance between two pinches is equal to the sheet length L_s, so the sheet can only be in one pinch at the same time. No slip is assumed between the sheet and the pinches and the coupling between the pinches and motors is assumed to be infinitely stiff. The mass of the sheet is assumed to be zero, which simplifies modeling of the sheet dynamics. The sheet position, defined as x_s, is assumed to be measured.

We adopt a hierarchical, cascaded control structure for the sheet feedback control design. This control layout consists of low level motor control loops and a high level sheet control loop for tackling disturbances and uncertainties at the motor level and at the sheet level, respectively. The control goal we adopt for the basic paper path case study is the design of stable and robust high level feedback controllers (HLCs) that track the desired reference trajectory. Regarding this reference motion task, possible choices are absolute reference tracking control and inter-sheet spacing control (Kruciński, 2000; Cloet, 2001). In this paper the first one is chosen and it is required that sheets are able to track a second-order sheet reference trajectory $x_{s,r}$.

The closed-loop linear motor dynamics in the Laplace domain can be represented by

$$\Omega_{Mi}(s) = T_i(s)\Omega_{Mi,r}(s), i \in \mathcal{I}, \qquad (1)$$

with $T_i(s)$ the complementary sensitivity function of controlled motor i, which maps the input of the low level closed-loop system (the motor reference velocity $\omega_{Mi,r}(t)$, with Laplace transform $\Omega_{Mi,r}(s)$), to its output (the actual motor velocity $\omega_{Mi}(t)$). Furthermore, $\mathcal{I} = \{1, 2, 3\}$ represents the index set of sheet regions. Since the bandwidth of the low level control loops is required to be significantly higher than the bandwidth of the high level control loop (Stephanopoulos, 1984), we

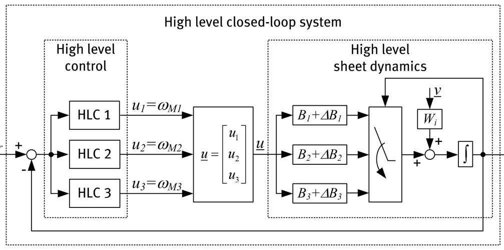

Fig. 3. Block diagram of the total control system.

assume perfect tracking behavior of the controlled motors, i.e., $T_i(s) = 1$, $\forall i \in \mathcal{I}$.

Under the assumption of ideal behavior in the low level control loop, the inputs u_i of the high level sheet dynamics will be directly generated by the HLCs. This is shown in Fig. 3, which represents the block diagram of the control system at hand. Since at each time instant the sheet is only driven by one pinch, the input of the sheet dynamics will change when the sheet arrives at the next pinch. This switching behavior can be easily captured in the PWL modeling formalism. The sheet velocity is derived from the motor velocities via straightforward holonomic kinematic constraint relations that describe the relation between motor velocity and pinch velocity, and pinch velocity and sheet velocity, respectively. The nominal high level sheet model, i.e. the sheet model without parameter uncertainties and disturbances, is:

$$\dot{x}_s = B_i \underline{u} \text{ for } x_s \in \mathcal{X}_i, i \in \mathcal{I}\,, \tag{2}$$

with the input matrices B_i defined as $B_1 = \begin{bmatrix} n_1 r_{P1} & 0 & 0 \end{bmatrix}$, $B_2 = \begin{bmatrix} 0 & n_2 r_{P2} & 0 \end{bmatrix}$, and $B_3 = \begin{bmatrix} 0 & 0 & n_3 r_{P3} \end{bmatrix}$, respectively. In these definitions, n_i represents the transmission ratio between motor i and pinch i and r_{Pi} represents the radius of the driven roller of pinch i. Furthermore, $\underline{u}$ is the column with inputs of the high level sheet dynamics: $\underline{u} = \begin{bmatrix} \omega_{M1} & \omega_{M2} & \omega_{M3} \end{bmatrix}^T$. The partitioning of the state space into the three regions is represented by $\{\mathcal{X}_i\}_{i\in\mathcal{I}} \subseteq \mathbb{R}$. Here, $\mathcal{X}_1 = \{x_s | x_s \in [x_{P1}, x_{P2})\}$, $\mathcal{X}_2 = \{x_s | x_s \in [x_{P2}, x_{P3})\}$, and $\mathcal{X}_3 = \{x_s | x_s \in [x_{P3}, x_{P3} + L_s)\}$.

In case parameter uncertainties and external disturbances are present, the high level PWL sheet model becomes:

$$\dot{x}_s = (B_i + \Delta B_i)\, \underline{u} + W_i \underline{v} \;\text{ for }\; x_s \in \mathcal{X}_i, i \in \mathcal{I}, \tag{3}$$

where ΔB_i is the constant uncertainty term of the i-th subsystem. In this model, this term can represent, for example, an uncertainty in the transmission ratio between motor i and pinch i or an uncertainty in the radius of the driven roller of pinch i. Column $\underline{v}$ acts as disturbances on the sheet velocity. These disturbances are scaled by the matrices W_i, defined as $W_1 = \begin{bmatrix} w_1 & 0 & 0 \end{bmatrix}$, $W_2 = \begin{bmatrix} 0 & w_2 & 0 \end{bmatrix}$, and $W_3 = \begin{bmatrix} 0 & 0 & w_3 \end{bmatrix}$, respectively.

3. ROBUST SHEET CONTROLLER DESIGN

In this section, we present the H_∞ controller synthesis method for the PWL sheet model (3), subject to uncertainties and disturbances. Since we are dealing with a tracking problem, the system is formulated in terms of its tracking error dynamics (Franklin *et al.*, 2002):

$$\begin{aligned} \dot{\underline{q}} &= F\underline{q} + (G_i + \Delta G_i)\, \underline{\mu} + V_i \underline{\nu} \\ &\quad \text{for } \left(x_{s,r} - \begin{bmatrix} 1 & 0 & 0 \end{bmatrix} \underline{q}\right) \in \mathcal{X}_i, i \in \mathcal{I} \\ z &= H\underline{q}. \end{aligned} \tag{4}$$

In this notation, the state vector $\underline{q}$ is defined as $\underline{q} = \begin{bmatrix} e_s & \dot{e}_s & \ddot{e}_s \end{bmatrix}^T$, with $e_s = x_{s,r} - x_s$ the tracking error. The control input $\underline{\mu}$ and the disturbance $\underline{\nu}$ are defined as $\underline{\mu} = \ddot{\underline{u}}$ and $\underline{\nu} = \ddot{\underline{v}}$, respectively. The system matrix is defined as $F = \begin{bmatrix} 0 & 1 & 0 \\ 0 & 0 & 1 \\ 0 & 0 & 0 \end{bmatrix}$, whereas the input matrix and the uncertainty term of the input matrix are defined as $G_i = \begin{bmatrix} 0_{3\times1} & 0_{3\times1} & -B_i^T \end{bmatrix}^T$ and $\Delta G_i = \begin{bmatrix} 0_{3\times1} & 0_{3\times1} & -(\Delta B_i)^T \end{bmatrix}^T$, respectively. Furthermore, the disturbance gain matrix and the output matrix in error space are defined as $V_i = \begin{bmatrix} 0_{3\times1} & 0_{3\times1} & -W_i^T \end{bmatrix}^T$ and $H = \begin{bmatrix} 1 & 0 & 0 \end{bmatrix}$, respectively. Regarding the uncertainty term ΔG_i, we make the assumption that its upper bound is known *a priori*:

$$[\Delta G_i]\, [\Delta G_i]^T \leq E_{Gi} E_{Gi}^T, i \in \mathcal{I}, \tag{5}$$

where E_{Gi} is a constant matrix satisfying (5) with the same dimensions as ΔG_i.

Given this notation in error space, the controller synthesis can be carried out. For this purpose, the approach presented in (Feng, 2002; Chen *et al.*, 2004) is slightly adjusted. Switching of the error dynamics from the one regime to the other does not depend on e, $\dot{e}$, or $\ddot{e}$, but on the sheet position x_s. As a result, using piecewise quadratic Lyapunov functions is not trivial for our tracking control case and, hence, we will use a common quadratic Lyapunov function in our analysis and synthesis.

The goal of the control design procedure is to find a feedback control law that stabilizes the uncertain PWL system (4). Furthermore, the controller should result in a guaranteed performance in the H_∞ sense. This means that, given a prescribed level of disturbance attenuation $\gamma > 0$, the induced L_2-norm of the operator from $\underline{\nu}$ to the controlled output z should be smaller than γ under zero initial conditions for all nonzero $\underline{\nu} \in L_2$ (Feng *et al.*, 2002; Feng, 2002; Chen *et al.*, 2004):

$$\|z\|_2 < \gamma \|\underline{\nu}\|_2. \tag{6}$$

In this case, the closed-loop error dynamics are said to be globally stable with disturbance attenuation γ. The control law we propose to realize the goal is based on static state feedback:

$$\underline{\mu} = -K\underline{q}. \tag{7}$$

Substitution of (7) into (4) yields the closed-loop error dynamics:

$$\begin{aligned} \dot{\underline{q}} &= A_{Ci}\underline{q} + V_i\underline{\nu} \\ &\quad \text{for } \left(x_{s,r} - \begin{bmatrix} 1 & 0 & 0 \end{bmatrix} \underline{q}\right) \in \mathcal{X}_i, i \in \mathcal{I}, \\ z &= H\underline{q}, \end{aligned} \tag{8}$$

with $A_{Ci} = F - (G_i + \Delta G_i) K$.

Given this closed-loop system, we can now present the following theorem for the controller design, which is based on Theorem 2 in (Chen *et al.*, 2004):

Theorem 3.1. Given a constant $\gamma > 0$, the PWL system (8) is globally stable with disturbance attenuation γ if the following matrix inequalities are satisfied:

$$0 < P = P^T \tag{9}$$

$$0 > \begin{bmatrix} \Omega_i & PH^T & Q^T \\ HP & -I & 0 \\ Q & 0 & -\epsilon I \end{bmatrix}, i \in \mathcal{I}, \tag{10}$$

with

$$\begin{aligned} \Omega_i &= PF^T + FP - Q^T G_i^T - G_i Q + \\ &\quad + \gamma^{-2} V_i V_i^T + \epsilon E_{Gi} E_{Gi}^T. \end{aligned} \tag{11}$$

Moreover, the controller gain for each subsystem is given by:

$$K = QP^{-1}. \tag{12}$$

For the proof of this theorem the reader is referred to (Chen *et al.*, 2004). As can be seen from Theorem 3.1, the conditions (9) and (10) are Linear Matrix Inequalities (LMIs) in the variables P, Q, ϵ, and γ^{-2}. This is in contrast with (Chen *et al.*, 2004), where products of ϵ and γ^{-2} exist. This results from the fact that we assume no uncertainty in the scaling matrix V_i of the disturbances.

4. EXPERIMENTAL SETUP

To experimentally validate the proposed control design approach, we use the paper path setup depicted in Figure 4. As can be seen in the figure, the setup consists of a PIM and a paper path with five pinches. In our experiments, only the second, third, and fourth pinch will be used. For the sake of notation, in the remainder of this paper we will refer to these pinches as pinch 1, pinch 2 and pinch 3, respectively. Each pinch is connected to a motor via a gear belt. The nominal transmission ratios between the motors and pinches are $n_1 = 0.49$, $n_2 = 0.47$, and $n_3 = 0.5$, respectively, and the pinch radii are $14 \cdot 10^{-3}$ m. The motors are 10 W DC motors, driven by power amplifiers with built-in current controllers. The angular positions of the motor shafts are measured using optical incremental encoders with a resolution of 2000 increments per revolution. Both the amplifiers and the encoders are connected to a PC-based control system. This system consists of a Pentium 4 host computer running RTAI/Fusion Linux and Matlab/Simulink and three TUeDACS USB I/O devices (van de Molengraft *et al.*, 2005). The sheets are guided through the paper path via thin steel wires and their position is measured using optical mouse sensors, which are directly connected to the host computer via USB.

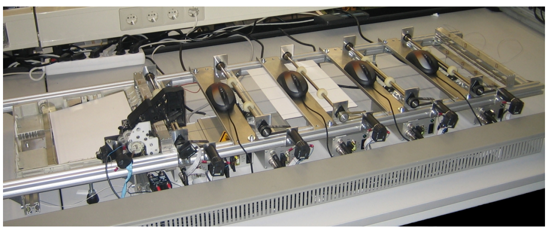

Fig. 4. The experimental paper path setup.

5. EXPERIMENTAL RESULTS

5.1 Control Design Results

To show the robustness against uncertain system parameters, the transmission ratios between the motors and pinches can be varied in the experimental setup. Besides the nominal ratios, a ratio of 0.53 can be implemented in the setup by changing the gear wheels. This results in maximum variations of the transmission ratios of $\Delta n_1 = 0.05$, $\Delta n_2 = 0.07$, and $\Delta n_3 = 0.03$, respectively. These variations will take the role of uncertain deviations from the nominal ratios. Given these deviations, the uncertainty terms ΔB_i in (3) become $\Delta B_1 = \begin{bmatrix} \Delta n_1 r_{P1} & 0 & 0 \end{bmatrix}$, $\Delta B_2 = \begin{bmatrix} 0 & \Delta n_2 r_{P2} & 0 \end{bmatrix}$, and $\Delta B_3 = \begin{bmatrix} 0 & 0 & \Delta n_3 r_{P3} \end{bmatrix}$, respectively. From ΔB_i, also the uncertainty terms on the input matrices of the open-loop error dynamics (4) can be calculated, which in turn are used to calculate the upper bounds on these terms according to (5), yielding $E_{Gi}E_{Gi}^T(k,l) = (\Delta n_i)^2 r_{Pi}^2$ for $k = l = 3$ and $E_{Gi}E_{Gi}^T(k,l) = 0$ for $k = l \neq 3$ and $k \neq l$, with k and l the row and column index, respectively. Given these matrices and by choosing $\gamma = 0.048$ the controller gain can be calculated according to Theorem 3.1:

$$K = 1 \cdot 10^5 \begin{bmatrix} -1.63 & -0.51 & -0.08 \\ -1.71 & -0.53 & -0.08 \\ -1.58 & -0.49 & -0.08 \end{bmatrix}. \tag{13}$$

The value of γ has been chosen such that the bandwidth of the high level control loop is significantly lower than the bandwidth of the low level control loops, as will be discussed in Section 5.2.

5.2 Low Level Motor Control

In this subsection, the low level control of motor 1 and its influence on the high level sheet dynamics is discussed. Although not shown, similar results were obtained for motors 2 and 3.

In the design procedure of the sheet feedback controllers we assumed perfect tracking behavior of the controlled motors, i.e. we assumed an infinite bandwidth of the motor control loops. Furthermore, we assumed an infinitely stiff coupling between the pinches and the motors. In a practical environment, however, these assumptions do not hold. Moreover, a digital implementation will cause a delay in the loop which will limit the attainable bandwidth. Based on identified motor dynamics, PID feedback controllers have been designed using loopshaping techniques (Franklin *et al.*, 2002). The controller parameters are tuned such that a bandwidth of 50 Hz has been realized. This can be seen in Figure 6, which depicts the Frequency Response Function (FRF) of the loopgain. Here, the bandwidth is defined as the frequency at which the 0 dB line of the open-loop FRF is crossed.

The rubber belt that connects the motor with the driven roller of the pinch has a limited stiffness, as can be observed from Figure 5, which shows the FRF of the transmission between motor 1 and pinch 1. It can be seen that the assumption on the infinite stiff coupling between motor and pinch only holds for frequencies up to approximately 100 Hz. In this frequency range, the measured transmission ratio coincides with the nominal transmission ratio of 0.49 (≈ -6.3) dB. For higher frequencies, the flexibility becomes dominant.

Given the high level sheet model and the HLCs, together with the controlled motor-pinch dynamics, the loopgain of the first subsystem can be derived. This loopgain is the transfer function

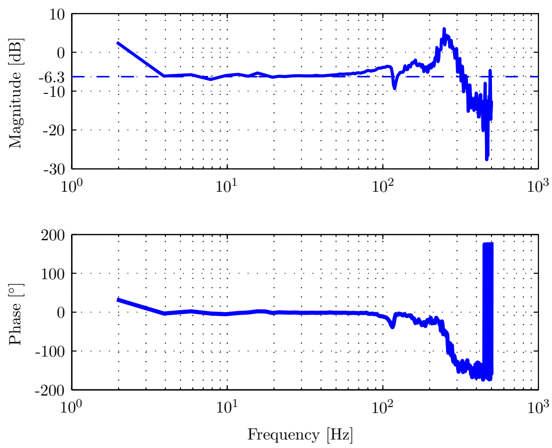

Fig. 5. FRF of the transmission between motor 1 and pinch 1 (solid), and the nominal transmission ratio (dashed)

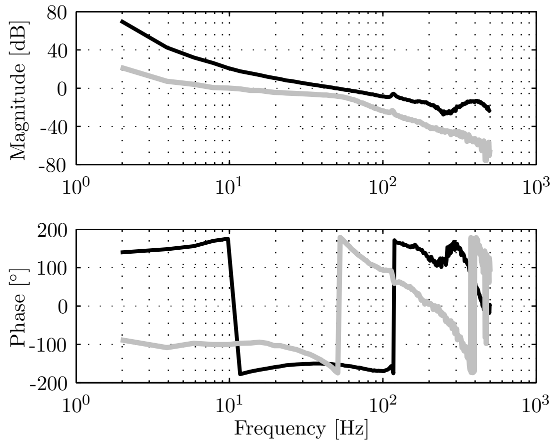

Fig. 6. FRF of the loopgain of the first motor control loop (black) and the FRF of loopgain of the first subsystem, including low level control (gray).

from the sheet tracking error to the actual sheet position. The FRF of this loopgain is also shown in Figure 6. It can be seen that a bandwidth of approximately 10 Hz has been realized. This is a factor 5 lower than the bandwidth of the motor control system, as required in a cascade control structure (Stephanopoulos, 1984). Furthermore, the phase lag at 10 Hz is approximately 90°. From this we can conclude that the first subsystem is stable.

In the control design procedure for the regulation of the PWL error dynamics, stability was proven for the case of perfect low level motor behavior. However, we want to apply the calculated controller (13) also in practical cases where we have to deal with non-ideal low level behavior, and still guarantee that the overall switched system is stable. In general, sheets have to be transported from the PIM to the FIN via the ITS (see Figure 1 and assume no backside printing) and the sheet reference velocity will be positive (Cloet *et al.*, 2001). To realize sequential switching in practice, we have to avoid negative actual sheet velocities to prevent the sheet from moving back to the previous pinch. Since the sheet control loops have a relatively low bandwidth and the sheet controllers can immediately respond to sheet tracking errors, negative sheet velocities are not likely to occur. Consequently, stability of the high level PWL system at hand is plausible in case of stable individual subsystems. So far, this reasoning has been approved by experimental results. However, a mathematically founded stability proof is subject of future research.

5.3 Validation Results

In the experimental validation of the control design, the focus is on the robustness of the system against parameter uncertainties. Therefore, the implemented transmission ratios are $n_1 = 0.49$, $n_2 = 0.53$, and $n_3 = 0.49$, i.e. the ratios of the second and third subsystem deviate from the nominal values. For the sheet motion task, a constant velocity of 0.27 ms^{-1} is chosen that has to be tracked throughout the entire paper path. The corresponding sheet reference motion $x_{s,r}$ is therefore a ramp function. Since no feedforward control input has been used, all three pinches are standing still until a sheet enters the first pinch. Due to the difference between the initial reference velocity and the actual initial velocity, the sheet error starts increasing when the sheet enters the first pinch, as can be seen in Figure 7. However, this error is decreased by the sheet controller in the first regime. It can be seen that some overshoot is present. Furthermore, it can be seen that the error increases when the sheet enters pinches two and three. This is due to the deviation of the transmission ratios with respect to the nominal values. Also these increases are controlled towards zero. From Figure 7, we can conclude that the closed loop system is stable and robust for parameter uncertainties within the specified bounds.

The difference between the experimentally obtained tracking error and the one obtained from simulation is also depicted in Fig. 7. It can be seen that there is a close match between both responses. This close match justifies the assumption on ideal low-level motor dynamics in the controller synthesis approach.

6. CONCLUSIONS AND FUTURE WORK

In this paper, a control design approach for robust sheet control in a printer paper path has been presented. The use of cheap optical mouse sensors as sheet position sensors has enabled the practical validation of the control design. Experiments show that a stable and robust closed-loop system has been obtained. This gives an opportunity in industrial applications to use less expensive mechanics with larger tolerances, and still to achieve the desired printing quality. Future research will focus on control design for cases in which pinches are coupled into sections, driven by one motor, and cases in which more than one pinch can influence the sheet motion. Furthermore, a mathematically founded stability proof of the total system in case of non-ideal motor control will be carried out.

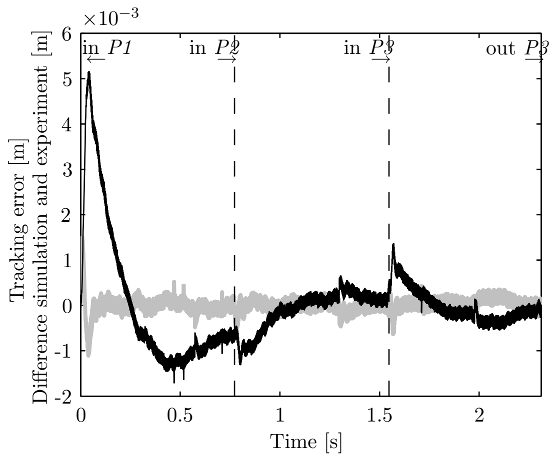

Fig. 7. Experimentally obtained sheet tracking error (black) and the difference in the responses obtained from simulation and experiment (gray).

REFERENCES

Chen, M., C.R. Zhu and G. Feng (2004). Linear-matrix-inequality-based approach to H_∞ controller synthesis of uncertain continuous-time piecewise linear systems. *IEE Proc.-Control Theory Appl.* **151(3)**, 295–300.

Cloet, Carlo (2001). *A Mechatronics Approach to Copier Paperpath Design.* Ph.D. thesis, University of California Berkeley, CA, USA.

Cloet, Carlo, Masayoshi Tomizuka and Roberto Horowitz (2001). Design requirements and reference trajectory generation for a copier paperpath. In: *Proceedings of the 2001 IEEE/ASME International Conference on Advanced Intelligent Mechatronics.* pp. 911–916.

Feng, Gang (2002). Controller design and analysis of uncertain piecewise-linear systems. *IEEE Trans. Circuits Syst. I* **49(2)**, 224–232.

Feng, Gang, G.P. Lu and S.S. Zhou (2002). An approach to H_∞ controller synthesis of piecewise linear systems. *Communications in Information and Systems* **2(3)**, 245–254.

Franklin, Gene F., J. David Powell and Abbas Emami-Naeini (2002). *Feedback control of dynamic systems.* Prentice Hall. Upper Saddle River, New Jersey, USA.

Kruciński, Martin (2000). *Feedback Control of Photocopying Machinery.* Ph.D. thesis, University of California Berkeley, CA, USA.

Rai, Sudhendu and Warren B. Jackson (1998). A hybrid hierarchical control architecture for paper transport systems. In: *Proc. of the* 37^{th} *IEEE Conference on Decision and Control.* Tampa, Florida, USA. pp. 4249–4250.

Stephanopoulos, George (1984). *Chemical Process Control.* Prentice Hall. Englewood Cliffs, New Jersey, USA.

van de Molengraft, René, Bram de Kraker and Maarten Steinbuch (2005). Integrating experimentation into control courses. *IEEE Control Syst. Mag.* **25(1)**, 40–44.